

Bis(fluoromesityl) Palladium Complexes, Archetypes of Steric Crowding and Axial Protection by *ortho* Effect – Evidence for Dissociative Substitution Processes – Observation of ^{19}F – ^{19}F Through-Space Couplings

Camino Bartolomé,^[a] Pablo Espinet,^{*[a]} Jose M. Martín-Álvarez,^[a] and Fernando Villafañe^[a]

Keywords: Palladium / Dissociative substitution / Fluorine / Bulky ligands / Steric crowding / Through-space coupling

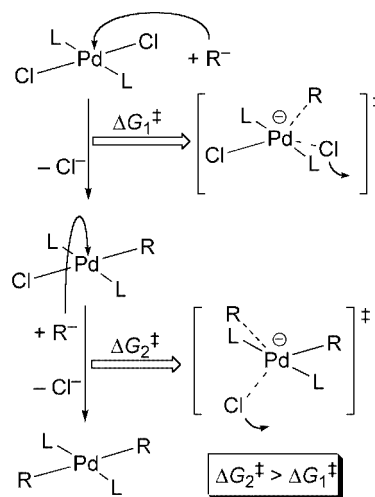
Bisarylated complexes $\text{trans}[\text{Pd}(\text{Fmes})_2(\text{SR}_2)_2]$ [Fmes = 2,4,6-tris(trifluoromethyl)phenyl (fluoromesityl); SR_2 = SMe_2 , tht ; tht = tetrahydrothiophene] are precursors for various bisarylated fluoromesityl palladium(II) complexes by ligand-substitution reactions. Boiling under reflux in acetonitrile gives the mixed complexes $\text{trans}[\text{Pd}(\text{Fmes})_2(\text{NCMe})(\text{SR}_2)]$, whereas boiling under reflux in toluene leads to $\text{trans}[\text{PdCl}_2\text{L}_2]$ (L = PMe_3 , $t\text{BuNC}$, $p\text{Tol-NC}$, 4-MePy), in the presence of neutral monodentate ligands, or to $(\text{NnBu}_4)[\text{trans-Pd}(\text{Fmes})_2\text{I}(\text{SR}_2)]$ when treated with $(\text{NnBu}_4)\text{I}$. $\text{trans}[\text{Pd}(\text{Fmes})_2(\text{SMe}_2)_2]$ reacts with bidentate ligands, also boiling under reflux in toluene, to give $[\text{Pd}(\text{Fmes})_2(\text{L-L})]$ [L-L = Me_2bipy , 2,2'-biquinoly, $\kappa^2\text{N,N'}$ - OCPy_2 , dppm ($\text{Ph}_2\text{PCH}_2\text{PPh}_2$), dppe ($\text{Ph}_2\text{PCH}_2\text{CH}_2\text{PPh}_2$), pte ($\text{PhSCH}_2\text{CH}_2\text{SPh}$), $\kappa^2\text{S,N}$ - SPPPh_2Py , $\kappa^2\text{O,N}$ - OPPhPy_2], or the bimetallic complex $[\text{Pd}(\text{Fmes})_2(\mu$

$1\kappa\text{N}:1,2\kappa\text{O}:2\kappa\text{N-Py}_2\text{MeCO})\text{Pd}(\text{Fmes})(\text{SMe}_2)]$ (characterized by X-ray diffractometry) when treated with $(\text{OH})(\text{CH}_3)\text{CPy}_2$. The crowding associated with two Fmes groups produces several interesting features: (1) *trans* complexes are preferred over *cis* complexes, against the expected electronic preferences; (2) the low-temperature NMR spectra of several complexes, or the X-ray diffraction structure of $[\text{Pd}(\text{Fmes})_2(2,2'\text{-biquinoly})]$, reveal significant structural distortions associated with steric crowding; (3) the need for boiling under reflux in the synthesis suggests a dissociative substitution mechanism, which is unknown so far for Pd; (4) some of the complexes show ^{19}F – ^{19}F through-space couplings.

© Wiley-VCH Verlag GmbH & Co. KGaA, 69451 Weinheim, Germany, 2004)

Introduction

2,4,6-Tris(trifluoromethyl)phenyl (nonafluoromesityl or Fmes) is an interesting ligand for main group and transition metals.^[1,2] It combines steric bulk with a certain electron-withdrawing character, and lacks hydrogens susceptible to H-elimination. The latter two features may facilitate the preparation of stable derivatives where the consequences (structural or otherwise) of steric crowding can be tested. However, its bulkiness limits direct arylation as a method of obtaining organometallics that contain more than one Fmes group. Our initial studies on the coordination of Fmes in palladium(II) complexes by arylation indicated that bisarylated complexes are only accessible for small ancillary ligands.^[2a] After the first arylation (Scheme 1), the coordinated Fmes exerts a high axial protection (*ortho* effect) against subsequent nucleophilic attack, which can progress reasonably well only when the spatial requirements of the ancillary ligands are small, so that the initially coordinated Fmes^- nucleophile. In kinetic terms, the activation enthalpy



Scheme 1. Associative mechanism for an arylation reaction

for the second arylation (ΔG_2^\ddagger) is noticeably higher than ΔG_1^\ddagger , its value increasing as the hindrance of the ancillary ligands to the tilting of the coordinated Fmes increases.

However, ligand substitution on bisarylated complexes obtained by arylation might allow the synthesis of a wider range of bisarylated species. Here we describe the synthesis and characterization of different bisarylated Fmes pal-

^[a] Departamento de Química Inorgánica, Facultad de Ciencias, Universidad de Valladolid, 47005 Valladolid, Spain
E-mail: espinet@qi.uva.es

ladium(II) complexes obtained by treating *trans*-[Pd(Fmes)₂(SR₂)₂] (SR₂ = SMe₂, tht; tht = tetrahydrothiophene) with monodentate or bidentate ligands. The reactions must be carried out in either toluene or acetonitrile boiling under reflux, suggesting a dissociative ligand substitution mechanism, which is unusual for Pd. Some of the *cis*-bisarylated complexes obtained show interesting structural features associated with their steric crowding. Several complexes exhibit ¹⁹F–¹⁹F through-space couplings between both Fmes. References on such couplings in organometallic compounds are scarce,^[3] even though many *cis*-bisarylated fluoroaryl complexes are known.^[4]

Results

Syntheses of Bisarylated Complexes

The complex *trans*-[Pd(Fmes)₂(SMe₂)₂] (**1a**) was obtained by arylation of *trans*-[PdCl₂(SMe₂)₂] with Li(Fmes), as described previously for *trans*-[Pd(Fmes)₂(tht)₂] (**1b**).^[2a] This complex is a better precursor for the preparation of other bisarylated complexes (Scheme 2) as SMe₂ has a higher volatility (b.p. 38 °C) than tht (b.p. 119 °C). Although in related Pd complexes (e.g. *trans*-[Pd(C₆F₅)₂(SMe₂)₂], or *trans*-[Pd(C₆F₅)₂(tht)₂]) SMe₂ or tht are easily displaced by other ligands at room temperature,^[4a] in these bis-Fmes de-

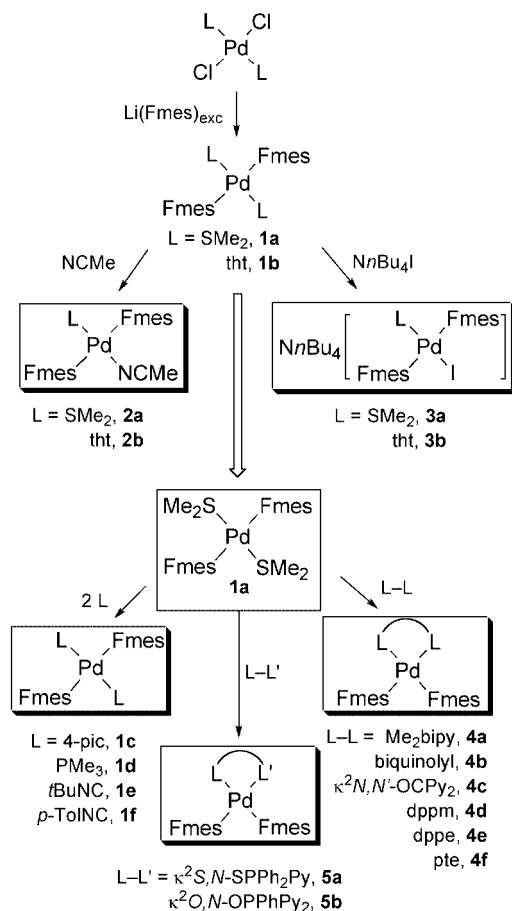
rivatives they resist displacement, even in the presence of a large excess of the entering ligand. Displacement is achieved only when the mixture is submitted to reflux in high-boiling temperature solvents such as toluene or MeCN.

Thus, neutral monodentate ligands L replace SMe₂ from **1a**, in refluxing toluene, to give the corresponding neutral mononuclear complexes *trans*-[Pd(Fmes)₂L₂] (L = 4-pic, **1c**; PMe₃, **1d**; *t*BuNC, **1e**, *p*Tol-NC, **1f**). The reactions do not proceed under milder conditions. Boiling under reflux **1a** or **1b** in NCMe produced *trans*-[Pd(Fmes)₂(NCMe)(SMe₂)] (**2a**).

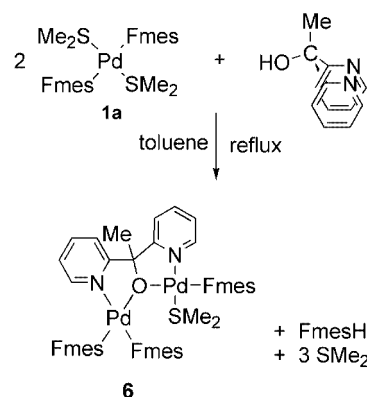
Treatment of **1a** or **1b** with excess (NnBu₄)I did not lead to the substitution of both thioether ligands by iodide, but to the formation of the monoanionic (NnBu₄)[*trans*-Pd(Fmes)₂I(SMe₂)] (**3a**) or (NnBu₄)[*trans*-Pd(Fmes)₂I(tht)] (**3b**), respectively.

Boiling under reflux in toluene was also required to replace the thioether ligands when **1a** was treated with neutral bidentate ligands L-L'. This produced [Pd(Fmes)₂(L-L)] (L-L = Me₂bipy (4,4'-Me₂-2,2'-bipyridine), **4a**; biquinolyl, **4b**; κ²N,N'-OCPh₂ (Py = 2-pyridyl), **4c**; dppm (Ph₂PCH₂PPh₂), **4d**; dppe (Ph₂PCH₂CH₂PPh₂), **4e**; pte (PhSCH₂CH₂SPh), **4f**).

Bisarylated complexes containing chemically non-equivalent Fmes groups were obtained with bidentate ligands containing two different donor atoms (L-L'). Thus the S,N-donor ligand SPPH₂Py gave [Pd(Fmes)₂(κ²S,N-SPPH₂Py)] (**5a**). Remarkably, equimolar amounts of **1a** and OPPhPy₂, which usually coordinates as κ²N,N-donor to Pd^{II},^[5] gave [Pd(Fmes)₂(κ²O,N-OPPhPy₂)] (**5b**). The treatment of (OH)(CH₃)CPy₂ with *trans*-[Pd(Fmes)₂(SMe₂)₂] (**1a**) did not afford the expected *cis* bisarylated complex, but gave instead the binuclear complex [Pd(Fmes)₂(μ-1κN:1,2κO:2κN-Py₂MeCO)Pd(Fmes)(SMe₂)] (**6**) (Scheme 3).



Scheme 2. Synthesis of the complexes



Scheme 3. Preparation of **6**

Characterization of Bisarylated Complexes

Solid-state IR spectra of all the bisarylated complexes show characteristic absorptions for the Fmes group.^[6] Absorption in the region 710–670 cm⁻¹ for several polyfluorophenyl has been associated with the R–M fragment and can be structurally informative: the *cis* isomers exhibit two

medium-to-strong bands in this range, whereas the *trans* isomers show only one.^[4a,7] This feature is also observed at 690–680 cm⁻¹ for the Fmes complexes, which supports their structural assignments. No additional evidence is provided by the IR data of **1a** (although the *trans* isomer was found in the structural determination of **1b**, previously reported),^[2a] and **1c**. The *trans* geometry for **1e** and **1f** is further supported by the presence of only one $\nu(\text{C}\equiv\text{N})$ absorption for the coordinated isocyanides.

trans-[Pd(Fmes)₂(*p*Tol-NC)₂] (**1f**) was characterized by solid-state X-ray diffractometry, as an example of a complex with a ligand with minimal steric requirements in the vicinity of the coordination sites. The molecular structure of **1f** (Figure 1) and selected distances and angles (Table 1) are given here.

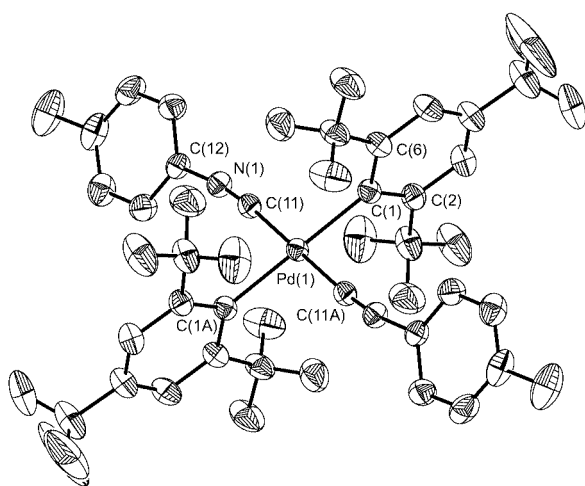


Figure 1. Molecular structure of *trans*-[Pd(Fmes)₂(*p*Tol-NC)₂] (**1f**). All hydrogen atoms omitted for clarity

Table 1. Selected bond lengths (Å) and angles (°) for *trans*-[Pd(Fmes)₂(*p*Tol-NC)₂] (**1f**); #1: $-x + 1, -y + 1, -z + 1$; #2: $-x, -y, -z$

Pd(1)–C(1)	2.102(4)	C(11)–Pd(1)–C(1)	92.80(14)
Pd(1)–C(11)	1.960(4)	C(11)–Pd(1)–C(1)#1	87.20(13)
C(11)–N(1)	1.152(5)	C(6)–C(1)–C(2)	114.4(3)
N(1)–C(12)	1.405(5)	C(22)–C(21)–C(26)	115.0(3)
Pd(2)–C(21)	2.098(4)	C(11)–N(1)–C(12)	171.5(4)
Pd(2)–C(31)	1.959(5)	C(31)–N(2)–C(32)	174.5(4)
C(31)–N(2)	1.152(5)	C(31)–Pd(2)–C(21)	91.93(15)
N(2)–C(32)	1.407(6)	C(31)#2–Pd(2)–C(21)	88.07(15)

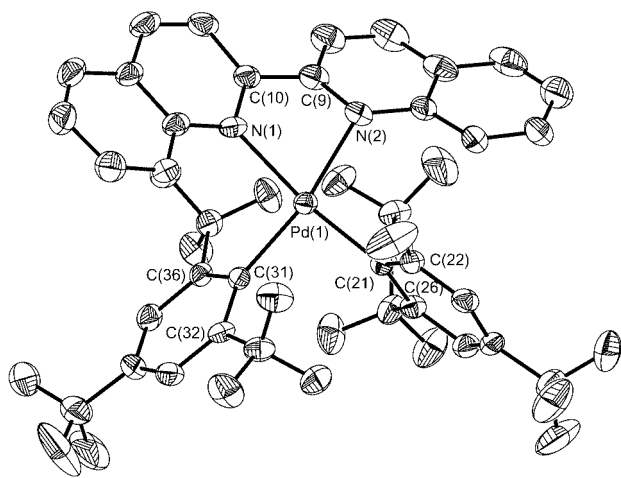
There are two independent molecules of **1f** in the unit cell, but only one-half of each molecule is included in the asymmetric unit. The molecules show a square-planar coordination for Pd, with the two isocyanide ligands in *trans* disposition (related by an inversion centre) and the isocyanide and the Fmes group forming an angle C(11)–Pd(1)–C(1) = 92.80(14)° in one molecule and C(31)–Pd(2)–C(21) = 91.93(15)° in the other. The two Fmes groups are coplanar and nearly perpendicular to the coordination plane, one showing the two Fmes groups tilted

only 5.8(4)° and the other 2.2(4)° to the coordination plane. The Pd–C_{ipso} distances [Pd(1)–C(1), 2.102(4) Å; Pd(2)–C(21), 2.098(4) Å] are similar to those found in *trans*-[Pd(Fmes)₂(tht)₂],^[2a] and somewhat longer than those in other complexes where the ligand *trans* to the Fmes is harder (see, for instance, other structures in this paper and in ref. 2). As usually observed in Fmes palladium complexes, the C–C–C angles at the *ipso* carbon are significantly less than 120° and those at the *ortho* carbon atoms are rather larger than 120° due to the electronic effects of the electropositive metal and electronegative CF₃ substituents at these positions.^[8] The C–N–C angle of the two isocyanide groups is < 180°, a common feature for isocyanides coordinated to transition metals.^[9] The structure suggests that there are no important repulsive interactions between neighbouring CF₃ groups, otherwise the rings would tilt to scatter these as much as possible. The elongation of the Pd–CF₃ distance compared with other complexes (and similar to *trans*-[Pd(Fmes)₂(tht)₂]) is then attributed mostly to a high *trans* influence of the Fmes group. Presumably, with these Pd–Fmes distances, there is little steric repulsion between facing CF₃ groups in a *trans*-[Pd(Fmes)₂L₂] complex.

The ¹⁹F NMR spectra of all the *trans* complexes **1** display two singlets with 2:1 intensities, except for **1d** where a triplet is observed for the *ortho*-CF₃ due to coupling with two equivalent phosphorus atoms. The *trans* geometry of complexes **2** and **3** is confirmed by the chemical equivalence of both Fmes groups.

The *cis* complexes **4** exhibit only one singlet for *para* CF₃ groups (which is consistent with the equivalence of the two Fmes groups), and another signal for the equivalent *ortho*-CF₃ groups. However, with biquinolyl **4b** and pte **4f** the latter signal is very broad, which is interpreted as owing to a slow concerted tilting of both Fmes groups, as observed for related systems.^[2a] The ¹H NMR spectra show that the two halves of the chelate ligands are equivalent through a C₂ axis.

To explore the expected distortions when more sterically demanding ligands are used, **4b** (L–L = 2,2'-biquinolyl) was characterized by solid-state X-ray diffractometry (Figure 2); Table 2 gives relevant distances and angles. The two Fmes ligands are coordinated in a *cis* arrangement, and the two N atoms of the biquinolyl ligand occupy the other coordination sites. The biquinolyl ligand is not planar, with the two halves forming an angle of 25.0(5)°. Moreover, the average plane of the biquinolyl ligand forms a dihedral angle of 35.8(5)° with the average coordination plane. This makes the nitrogen atoms pyramidal, as found in [Pd(biquinolyl)(allyl)]⁺ complexes.^[10] The square-planar geometry of Pd is severely distorted towards tetrahedral with the C_{ipso} atoms of the two Fmes situated 0.42 and 0.98 Å above and below, respectively, the N–Pd–N plane. For comparison, the related complex [Pd(Fmes)₂(bipy)], which is also tetrahedrally distorted,^[2a] shows a smaller distortion with the C_{ipso} atoms 0.40 Å above and below the N–Pd–N plane. Tetrahedral distortion is associated with angles that differ greatly from those expected for a square-planar geo-

Figure 2. Molecular structure of [Pd(Fmes)₂(biquinoyl)] (**4b**)Table 2. Selected bond lengths (Å) and angles (°) for [Pd(Fmes)₂(biquinoyl)] (**4b**)

Pd(1)–C(21)	2.014(6)	C(21)–Pd(1)–C(31)	93.9(2)
Pd(1)–C(31)	2.056(5)	C(21)–Pd(1)–N(2)	100.46(19)
Pd(1)–N(1)	2.136(5)	C(31)–Pd(1)–N(1)	94.83(19)
Pd(1)–N(2)	2.248(4)	N(1)–Pd(1)–N(2)	75.88(18)
		C(26)–C(21)–C(22)	113.8(5)
		C(36)–C(31)–C(32)	113.5(5)

metry: C(21)–Pd(1)–C(31) 93.9(2)°; C(21)–Pd(1)–N(2) 100.46(19)°; C(31)–Pd(1)–N(1) 94.83(19)°. The N(1)–Pd(1)–N(2) angle is 75.88(18)°, a normal value for this small-bite chelating ligand. Despite these distortions the Pd–C and Pd–N distances are not affected noticeably, remaining very similar to those of the square-planar [Pd(bipy)(Fmes)₂].^[2a]

κ^2O,N -Coordination of OPPhPy₂ in **5b** is supported by the phosphorus chemical shift in the ³¹P{¹H} NMR spectrum, which clearly differs from those shifts when OPPhPy₂ acts as κ^2N,N -donor (Table 3), and is closer to those of the κ^2O,N -chelate OPPh₂Py.^[2c,5,11] The difference with the latter can be accounted for by the higher shielding effect on P of Py compared with Ph. The P–O stretching absorptions are usually useful in differentiating κ^2O,N - and κ^2N,N -coordination modes of OPPhPy₂^[12] but this band is not detected in the IR spectrum of **5b** due to other intense absorptions in the same range.

Table 3. ³¹P NMR chemical shifts of 2-pyridylphosphane oxide and bis(2-pyridyl)phosphane oxide palladium complexes, at room temperature in CDCl₃

Complexes	Coordination mode	δ [ppm]	Ref.
[Pd(Fmes) ₂ (OPPhPy ₂)] (5b)	κ^2O,N	39.01	this work
[Pd(C ₆ F ₅) ₂ (OPPh ₂ Py)]	κ^2O,N	49.8	[5]
[Pd(C ₆ F ₅)Br(OPPh ₂ Py)]	κ^2O,N	49.9	[5]
[Pd(Fmes)(NCMe)(OPPhPy ₂)]BF ₄	κ^2N,N	21.1	[11]
[PdCl(Fmes)(OPPhPy ₂)]	κ^2N,N	20.4	[2c]
[Pd(C ₆ F ₅)X(OPPhPy ₂)]	κ^2N,N	20.7–21.0	[5]
[Pd(C ₆ F ₅) ₂ (OPPhPy ₂)]	κ^2N,N	20.7	[5]

Unequivocal characterization of [Pd(Fmes)₂(μ -1 κN :1,2 κO :2 κN -Py₂MeCO)Pd(Fmes)(SMe₂)] (**6**) required an X-ray diffraction study. A perspective view of the molecular structure is given in Figure 3, and selected distances and angles are listed in Table 4.

The complex is binuclear and the two Pd coordination planes make a dihedral angle of 72.1(4)° (Figure 3). The molecule contains three non-equivalent Fmes groups, two

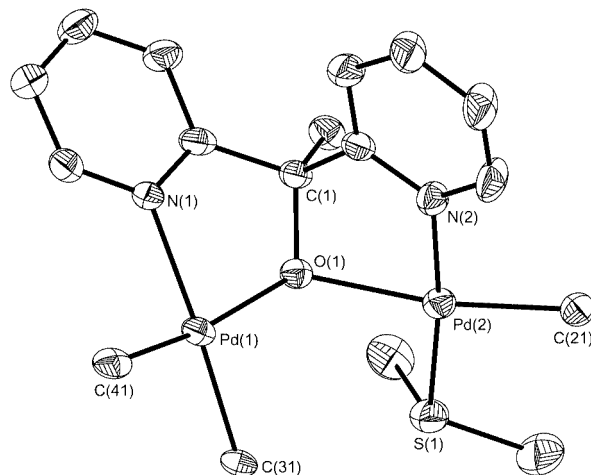
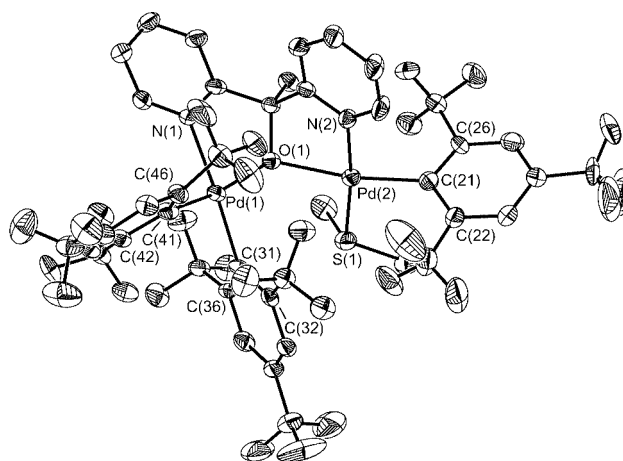
Figure 3. (top) Molecular structure of [Pd(Fmes)₂(μ -1 κN :1,2 κO :2 κN -Py₂MeCO)Pd(Fmes)(SMe₂)] (**6**); (bottom) view of the skeleton showing the mode of coordination of the [O(CH₃)CPy₂][–] ligand

Table 4. Selected bond lengths (Å) and angles (°) for [Pd(Fmes)₂(μ-1κN:1,2κO:2κN-Py₂MeCO)Pd(Fmes)(SMe₂)](C₆H₅CH₃)_{0.5} (**6**·0.5 toluene)

Pd(1)–C(41)	2.011(13)	C(31)–Pd(1)–N(1)	167.3(4)
Pd(1)–C(31)	2.027(10)	C(41)–Pd(1)–O(1)	168.4(4)
Pd(1)–N(1)	2.101(8)	C(21)–Pd(2)–N(2)	92.4(4)
Pd(1)–O(1)	2.147(6)	N(2)–Pd(2)–O(1)	79.5(3)
Pd(2)–C(21)	2.005(11)	C(21)–Pd(2)–S(1)	94.2(3)
Pd(2)–N(2)	2.049(10)	O(1)–Pd(2)–S(1)	93.9(2)
Pd(2)–O(1)	2.122(7)	N(2)–Pd(2)–S(1)	173.3(3)
Pd(2)–S(1)	2.290(4)	C(21)–Pd(2)–O(1)	170.7(3)
C(41)–Pd(1)–C(31)	95.6(4)	C(26)–C(21)–C(22)	115.5(12)
C(41)–Pd(1)–N(1)	91.8(4)	C(36)–C(31)–C(32)	113.7(10)
C(31)–Pd(1)–O(1)	93.6(3)	C(46)–C(41)–C(42)	111.8(11)
N(1)–Pd(1)–O(1)	80.4(3)		

of them *cis* coordinated to one of the metal centres, Pd(1). Each pyridyl group of the [O(CH₃)CPy₂][–] ligand is coordinated to a different palladium atom, whereas the oxygen atom bridges the two metal centres. The SMe₂ ligand occupies the fourth coordination site in the monoarylated Pd atom.

The Pd–C distances are all very similar [Pd(1)–C(41) 2.011(13), Pd(1)–C(31) 2.027(10), Pd(2)–C(21) 2.005(11) Å], lying in the range of other *cis* bisarylated or monoarylated Fmes Pd complexes.^[2a–2c] The distances and angles of the [O(CH₃)CPy₂][–] ligand are similar to those found in In^{III} [13] and Cu^{II} [14] complexes, where it is also coordinated as a bridging ligand.

Whereas the geometry of the monoarylated palladium centre is nearly square planar, that of the bisarylated palladium centre is very distorted, since N(1) is 0.574(15) Å out of the plane defined by O(1)–C(41)–Pd(1)–C(31). The N(1)–Pd(1)–O(1) and N(2)–Pd(2)–O(1) angles are significantly lower than 90° [80.4(3)° and 79.5(3)°], which is compensated for by the C(31)–Pd(1)–O(1) and O(1)–Pd(2)–S(1) angles [93.6(3)° and 93.9(2)°, respectively]. The *cis* angle involving the carbon atoms of the Fmes ligands is larger than 90° [95.6(4)°], presumably as a result of steric constraints.

The Fmes groups are not perpendicular to the coordination plane, but tilted in the same sense by 70.4° [C(41)], 64.6° [C(31)] and 78.6° [C(21)]. This tilting, observed for other *cis* bis(Fmes) palladium complexes,^[2a] seems to help in minimizing the repulsions between the *ortho*-CF₃ substituents of *cis* Fmes groups.

¹⁹F NMR spectra of complexes **5a**, **5b**, and **6** reveal ¹⁹F–¹⁹F through-space coupling (see below).

Discussion

For square-planar aryl complexes, although the C–M bonding interaction is little affected by the dihedral angle between the aryl and the coordination plane, the aryl groups tend to lie perpendicular to the coordination plane to minimize steric repulsions.^[15] Conversely, ligand-substitution reactions on 16e palladium(II) complexes follow an

associative mechanism via 18e pentacoordinate transition states, rather than the alternative dissociative pathway via 14e three-coordinate intermediates.^[16] We know of no exception to this rule for palladium, although several dissociative ligand substitution have been found in bis(aryl) derivatives of platinum.^[17] The aryl complexes reported here show dramatic deviations from the normal behaviour of Pd^{II} complexes due to the steric crowding produced by the four *ortho*-CF₃ groups competing for the same axial space over the coordination plane. It is convenient to discuss first their structural features to better understand their reactivity. Fortunately, many results for these bis(Fmes) complexes can be directly compared with those in the literature for C₆F₅ complexes, and with the mono(Fmes) complexes recently reported.^[2c]

Structures in the Solid State and in Solution

(A) Complexes *trans*-[Pd(Fmes)₂L₂] (L = monodentate ligand): X-ray structures of the complexes with L = tht,^[2a] *p*Tol-NC show an essentially square-planar geometry, with the Fmes rings almost coplanar and perpendicular to the coordination plane. The same arrangement has been found in the square planar *trans*-[Au(Fmes)₂L₂][–].^[1f] However, in the linear complex [Au(Fmes)₂][–] the aryl planes of the two Fmes groups make an angle of 27.2°. For comparison, the complex [Au(C₆F₅)₂][–] shows coplanar rings.^[18] Thus, two *trans* Fmes groups are better stabilized as coplanar and lay perpendicular to the coordination plane when the other two positions in the square-planar geometry are occupied. When there are no ancillary ligands present, as in [Au(Fmes)₂][–], the Fmes groups scatter by rotation, giving rise to a pseudohelicoidal geometry and relieving the repulsion between the facing *ortho*-CF₃ groups. Such behaviour suggests that the steric repulsion between two *trans* Fmes groups is perceptible but very moderate.

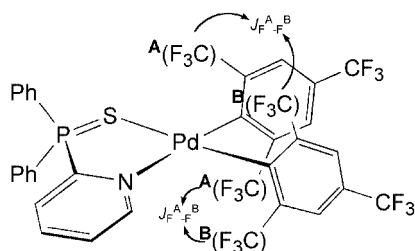
(B) Complexes *cis*-[Pd(Fmes)₂(L-L')] [L-L = bipy,^[2a] biquinoyl (4b**), or the *cis*-bisarylated moiety of **6**]:** These square-planar geometries are clearly more distorted towards tetrahedral than those of *trans* bisarylated complexes. The distortion increases with the size of the ancillary ligands. The Pd–C distances are shorter than for the *trans* bisarylated complexes (the *trans* effect of the ancillary ligands is lower than that of Fmes), and slightly longer than those in monoarylated Fmes Pd complexes (the latter are usually below 2.0 Å).^[2c] The Fmes groups are not perpendicular to the coordination plane, as is usual in common aryl derivatives, but tilted in the same sense by ca. 20° from the perpendicular. Since the steric crowding in a *cis* bisarylated moiety is clearly higher than in *trans* bisarylated complexes, so must be the corresponding repulsions. This concerted tilt appears to be the best distortion to minimize repulsions between the *ortho*-CF₃ of the two contiguous Fmes ligands, even if it increases the repulsions with the ancillary ligands. This distortion should make chemically non-equivalent the *exo* and *endo* (relative to the C–Pd–C angle) *ortho*-CF₃ groups. In solution all the *cis* bisarylated complexes reported here are stereochemically dynamic, and a concerted tilting of the two Fmes ligands gives rise to an

averaged geometry in which the Fmes groups would be perpendicular to the coordination plane. The barrier to this *endo-exo* exchange is low, but a broadening of the *ortho*-CF₃ signals is observed in the low-temperature ¹⁹F NMR spectra of some of the *cis* bisarylated complexes. The tilting has been frozen out in the recently reported related Ni complex [Ni(Fmes)₂(1,2-dimethoxyethane)₂],^[19] where the smaller metal atom leads to greater crowding.

No spectroscopic evidence was found in solution for the tetrahedral distortion observed in the solid-state structures of some of the complexes. For instance, the ¹⁹F NMR of **4b** should give four *ortho*-CF₃ signals if the solid-state structure were “frozen” in solution, but only one signal is observed. This indicates that the barriers for the process averaging the coordination plane and that for the concerted tilting are low, and that the processes are fast even at low temperatures.

(C) Complexes *cis*-[Pd(Fmes)₂(L-L')] with Other Chelating Ligands. ¹⁹F–¹⁹F Through-Space Couplings: Complexes **5a**, **5b**, and **6** have less symmetric structures and their spectra reveal ¹⁹F–¹⁹F through-space couplings between close non-equivalent *ortho*-CF₃ groups. The *para*-CF₃ groups are too far away to show through-space coupling.

In [Pd(Fmes)₂(SPPPh₂Py)] (**5a**) the ligand SPPPh₂Py coordinates to the bisarylated fragment as a κ²S,N-donor in an averaged planar chelate ring (Scheme 4). The fast envelope-shift movement of the five-membered chelate rings has a very low activation energy, allowing us to consider the five-membered metallacycle as planar.^[20] Accordingly, the ¹⁹F NMR spectrum of **5a** shows two high-field singlets due to the two non-equivalent *para*-CF₃, whereas the *ortho*-CF₃ groups form a X₃A₃A'₃X'₃ system, which affords two quadruplets, with *J* = 9.3 Hz. This value may be ascribed to through-space coupling between the fluorine atoms on the same side of the coordination plane (Scheme 4), as there are too many bonds between the inequivalent atoms to permit significant scalar coupling, and the coupling constant is similar to those detected in some fluoroaryl complexes described by our group.^[3] No diagonal coupling is detected between CF₃ groups of different Fmes groups, nor between different CF₃ groups at opposite sides of the coordination plane.



Scheme 4. ¹⁹F–¹⁹F through-space couplings in **5a**

In [Pd(Fmes)₂(κ²O,N-OPPhPy₂)] (**5b**) the ligand OPPhPy₂ coordinates to the bisarylated moiety as κ²O,N-donor (Scheme 6). As for **5a**, the inequivalent *para*-CF₃ give

rise to two high-field singlets, whereas the *ortho*-CF₃ groups now constitute an A₃K₃M₃X₃ system, giving rise to four quadruplets. The coupling constants (7.5, 6.0 Hz) are similar to those of **5a**, indicating that the observed through-space coupling occurs between *ortho*-CF₃ groups in different Fmes rings, but at the same side of the coordination plane. As before, no other couplings are detected.

For [Pd(Fmes)₂(μ-1κN:1,2κO:2κN-Py₂MeCO)Pd(Fmes)(SMe₂)] (**6**) the ¹⁹F NMR spectrum shows three singlets in the *para*-CF₃ region, confirming the presence of three non-equivalent Fmes groups. Six signals (one singlet and five multiplets) are detected in the *ortho*-CF₃ region (Figure 4), indicating that they are all non-equivalent. Homonuclear decoupling experiments allowed us to assign which nuclei are involved in each coupling (Figure 4), assuming that all the coupling constants observed are due to through-space coupling between fluorine atoms on the same side of the coordination planes, as observed for **5a** and **5b**. While F₃C(29) appears as non-coupled because it is far from the rest of fluoromethyl groups, F₃C(37) is coupled with F₃C(49) (both on the same metal) and with F₃C(27) (which is on the other Pd atom). The coupling constants are 10 and 8.5 Hz, respectively. The other two fluoromethyl groups showing couplings are F₃C(47) and F₃C(39), with *J* = 8 Hz. These through-space coupling constants give an estimation of the distance between the fluoromethyl groups;^[21] the higher coupling the shorter distance, regardless of whether the fluoromethyl groups belong to Fmes coordinated to the same or to different metal centres.

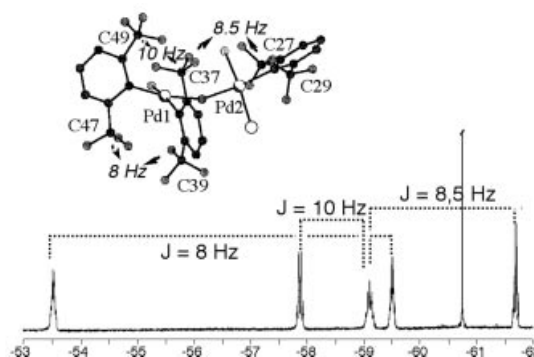


Figure 4. ¹⁹F NMR of [Pd(Fmes)₂(μ-1κN:1,2κO:2κN-Py₂MeCO)Pd(Fmes)(SMe₂)] (**6**) (*ortho*-CF₃) in CDCl₃ at 298 K, showing the through-space couplings observed

Complex **6** shows a slow dynamic process in solution that involves the SMe₂ group. Its ¹H and ¹⁹F spectra in CDCl₃ at room temperature accord with the solid-state structure, but the two signals for the methyl groups of the SMe₂ are broad at room temperature, and coalesce at 333 K. This equivalence can be achieved by a process requiring both inversion of the sulfur atom and rotation about the Pd–S bond. The high steric crowding could be responsible for the very slow exchange at room temperature. However, a process involving SMe₂ dissociation and reassociation occurs

for other isomerizations in complexes with this weakly bound ligand^[3b] and can not be discounted here.

Mechanisms of the Syntheses of Bisarylated Complexes

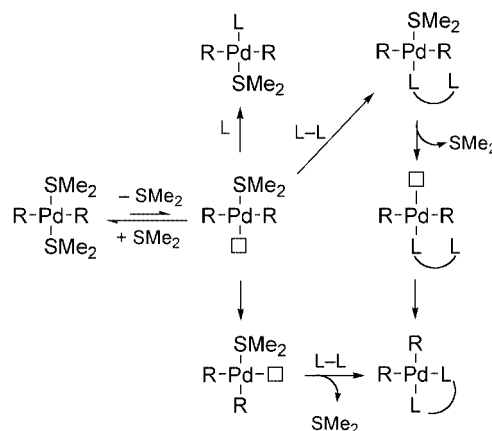
In contrast with the reaction features of ligand substitution in $[\text{PdCl}(\text{Fmes})\text{L}_2]$ complexes, which suggest an associative mechanism,^[2c] the harsh conditions required for ligand substitution in the bis-Fmes complexes suggest a dissociative mechanism, implying a positive activation entropy, which is favoured at high temperature.^[22] Although associative ligand substitutions dominate palladium(II) chemistry (so far they are the only type observed), dissociative mechanisms could become competitive (faster) as the associative are disfavoured. Dissociative ligand substitution could be favoured by (i) PdR_2 substrates where R is a good σ -donor;^[23] (ii) complexes with bulky ligands;^[17e,22] and (c) substrates with labile leaving ligands. These three requirements are met by **1a**. An associative mechanism through a five-coordinate transition state should be disfavoured in our system for electronic reasons (the palladium centre in bisarylated substrates is electron rich), and even more so for steric reasons: as the z axis is occupied above and below the metal coordination plane by the *ortho*- CF_3 of the two Fmes groups, the attack of even a small nucleophile looks to be extremely difficult (*ortho* effect).

This leads us to propose the mechanism depicted in Scheme 5 for the substitution reactions. The formation of only *trans* bis-Fmes complexes from the reactions of *trans*- $[\text{Pd}(\text{Fmes})_2(\text{SMe}_2)_2]$ with monodentate ligands contrasts with previous observations for reactions on *trans*- $[\text{Pd}(\text{C}_6\text{F}_5)_2(\text{tht})_2]$, where *cis* complexes are formed in preference.^[22b] This means that *trans*- $[\text{Pd}(\text{Fmes})_2\text{L}_2]$ and *cis*- $[\text{Pd}(\text{C}_6\text{F}_5)_2\text{L}_2]$ are the thermodynamic products, respectively, for these two aryls. Formation of the *trans* isomer with Fmes complexes occurs against the antisymbiotic effect (or transphobia),^[24] indicating that the relief of steric crowding in the *trans* complex compensates for the higher electronic destabilization associated with two *trans* Fmes groups.

Boiling under reflux complexes **1** in NCMe furnishes *trans*- $[\text{Pd}(\text{Fmes})_2(\text{NCMe})(\text{SR}_2)]$ (**2**) complexes. The bis(aceetonitrile) complex $[\text{Pd}(\text{Fmes})_2(\text{NCMe})_2]$ has not been detected, suggesting that the first substitution of SMe_2 by the poorer donor NCMe makes the complex less electron rich, and the dissociation of a second SR_2 becomes disfavoured.

The formation of the monosubstituted products, $(\text{NnBu}_4)[\text{trans-Pd}(\text{Fmes})_2\text{I}(\text{SR}_2)]$ (**3**), after the reactions of *trans*- $[\text{Pd}(\text{Fmes})_2(\text{SR}_2)_2]$ (**1**) with $(\text{NnBu}_4)\text{I}$ can be considered normal. The formation of $(\text{NnBu}_4)_2[\text{Pd}(\text{Fmes})_2\text{X}_2]$ is, apparently, counter-thermodynamic; similar results have been found for non-crowded bisarylated complexes. For instance, no $[\text{Pd}(\text{C}_6\text{F}_5)_2\text{X}_2]^{2-}$ complexes have been reported, despite many studies on (pentafluorophenyl)palladium complexes.^[25]

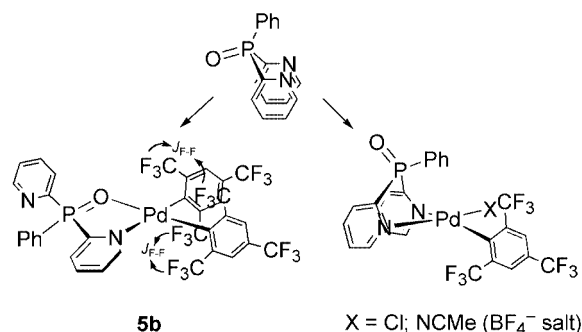
The formation of complexes **4** and **5** involves a *trans*-to-*cis* isomerization from the starting material to the final product. Thus, a topomerization of the *trans* to the corresponding *cis* three-coordinate intermediate is needed



Scheme 5. Dissociative mechanism of the substitution processes

(Scheme 5). Thermodynamically, the “chelate effect”, and in most cases the use of a stronger ligand, contribute to compensate the destabilization caused by the higher repulsion between two *cis* Fmes groups. In addition, the first dissociative substitution by a better σ -donor with a higher *trans* influence (except for the ligand pte, where the change is *S*-donor for *S*-donor), favors, kinetically, the dissociation of the second SR_2 ligand.

The $\kappa^2\text{O},N$ -coordination of OPhPy_2 found in **5b** was unknown for square-planar palladium(II), although it occurs in pseudo-octahedral molybdenum(II) derivatives.^[26] κ^2N,N -Coordination usually observed in Pd^{II} complexes is probably disfavoured in our case by the high degree of steric crowding due to the presence of two *cis* Fmes groups, quite similarly to its prevention in octahedral complexes. The $\kappa^2\text{O},N$ -coordination takes the substituents of the phosphorus away from the axial positions, minimizing the steric congestion. Interestingly, monoarylated complexes $[\text{PdCl}(\text{Fmes})(\kappa^2N,N\text{-OPhPy}_2)]$ and $[\text{Pd}(\text{Fmes})(\text{NCMe})(\kappa^2N,N\text{-OPhPy}_2)]\text{BF}_4$ have been isolated and characterized.^[2c,11] Therefore, one Fmes group is compatible with an axial disposition of the phenyl group in κ^2N,N -coordination, but two Fmes groups (here) or an octahedral metal centre (Mo complex cited above) force $\kappa^2\text{O},N$ -coordination. This highlights the very different “axial” encumbrance produced in monoarylated and bisarylated Fmes complexes. In monoarylated derivatives the Fmes group is probably tilted to accommodate the phenyl group (Scheme 6). The ability



Scheme 6. Bisarylated (indicating detected ^{19}F – ^{19}F through-space coupling) and monoarylated OPhPy_2 complexes

of Fmes to tilt and make the space in the *z* direction accessible to attack by nucleophiles explains why the reactions involving monoarylated substrates can proceed by associative mechanisms,^[2c] while those reported here seem to require ligand dissociation.

We used a ligand with smaller substituents, (OH)(CH₃)CPy₂, to check whether κ^2N,N -coordination occurred, but this yielded, unexpectedly, [Pd(Fmes)₂(μ -1 κN :1,2 κO :2 κN -Py₂MeCO)Pd(Fmes)(SMe₂)] (**6**), and HFmes as by-product (Scheme 3). The alcoholic hydrogen has been previously reported to be acidic when the ligand is coordinated to other metals, such as In^{III}.^[13] However, no deprotonation occurred during the reactions of (OH)(CH₃)CPy₂ with the monoarylated complexes *trans*-[PdClFmes(SMe₂)₂] or [Pd(Fmes)(NCMe)₃]BF₄, which lead to [PdClFmes(κ^2N,N' -(OH)(CH₃)CPy₂)]^[2c] and [Pd(Fmes)-{ κ^2N,N' -(OH)(CH₃)CPy₂}(NCMe)]BF₄, respectively.^[11] This suggests that acidic activation of the O–H bond might require previous *O*-coordination to a putative three-coordinate palladium intermediate. This might occur in the dissociative mechanism for bisarylated complexes but not in the associative substitution operating for monoarylated species.^[2c]

Conclusion

Substitution and isomerization processes in bisarylated Fmes palladium complexes seem to occur by dissociative mechanisms, forced by the extreme axial protection produced by the *ortho* CF₃ substituents (*ortho* effect). Consequently, harsh reaction conditions are required, unlike the mild substitution by associative mechanisms found for the related monoarylated Fmes complexes,^[2c] or for the analogous bisarylated C₆F₅ complexes.^[5]

The lesser steric repulsion of two bulky Fmes mutually *trans*-stabilizes better the *trans* isomers, which should not be the thermodynamic products on the basis of only electronic effects (“antisymbiotic effect” or transphobia); *cis* isomers are obtained only for bidentate ancillary ligands, due to the chelate effect.

The ¹⁹F–¹⁹F couplings observed have no significant scalar contribution, and are due to through-space coupling that depends on the distance between the interacting nuclei. This is clearly so as the magnitude of the coupling does not depend on whether the fluoromethyl groups are on Fmes coordinated to the same metal or on Fmes coordinated to different metals in a binuclear complex.

Experimental Section

General Remarks: All reactions were carried out under dry N₂. Solvents were purified according to standard procedures.^[27] The complexes *trans*-[PdCl₂(tht)₂], *trans*-[PdCl₂(SMe₂)₂],^[28] *trans*-[Pd(Fmes)₂(tht)₂] (**1b**)^[2a] and the ligands OPPhPy₂,^[29] SPPh₂Py,^[30] and (OH)(CH₃)CPy₂,^[31] were prepared according to literature procedures. *p*Tol-NC was synthesized as reported^[32] using triphosgene as dehydrating agent.^[33] 1,3,5-C₆H₃(CF₃)₃ (FmesH) from Fluoro-

chem was used as received, and Li(Fmes) was prepared in situ as described in the literature.^[34] The rest of the reactants were purchased from commercial suppliers and used as received.

Infrared spectra were recorded with a Perkin–Elmer 883 apparatus as Nujol mulls between polystyrene films from 4000 to 200 cm^{−1}. NMR spectra were recorded with Bruker AC-300 or ARX-300 instruments. ¹H, ³¹P{¹H} and ¹⁹F NMR spectra are referenced to TMS, 85% aqueous H₃PO₄, and CFC₃, respectively. Elemental analyses were performed with a Perkin–Elmer 2400B microanalyzer.

***trans*-[Pd(Fmes)₂(SMe₂)₂] (**1a**):** *trans*-[PdCl₂(SMe₂)₂] (0.604 g, 2 mmol) was added to a freshly prepared solution of Li(Fmes) (7.95 mmol) in Et₂O (40 mL). The reaction mixture was maintained at 40 °C for 24 h, and then two drops of water were added to hydrolyse the excess organolithium reagent. The volatiles were pumped off, and the residue was extracted with toluene and filtered through silica gel. The solvent was then evaporated and the resultant pale brown residue was recrystallized from dichloromethane/hexane at −20 °C to give pale yellow crystals that were decanted, washed with hexane and vacuum-dried. Yield 0.801 g (51%). IR: $\tilde{\nu}$ = 687 s cm^{−1}. ¹⁹F NMR: δ = −63.18 (s, 6 F, *para*-CF₃), −60.41 (s, 12 F, *ortho*-CF₃) ppm. ¹H NMR: δ = 1.66 [s, 12 H, S(CH₃)₂], 7.92 [s, 4 H, C₆H₂(CF₃)₃] ppm. C₂₂H₁₆F₁₈PdS₂ (792.86): calcd. C 33.33, H 2.03; found C 33.16, H 2.03.

***trans*-[Pd(Fmes)₂(4-pic)₂] (**1c**):** 4-pic (21.4 μ L, 0.021 g, 0.22 mmol) was added to a solution of **1a** (0.080 g, 0.1 mmol) in toluene (10 mL) and boiled under reflux for 3 h. The so-obtained solution was filtered through dry Celite, the volatiles were pumped off, and the resultant white solid was washed with hexane and vacuum dried [yield 0.055 g (65%)]. Recrystallization from dichloromethane/hexane gave colourless crystals. IR: $\tilde{\nu}$ = 688 m cm^{−1}. ¹⁹F NMR: δ = −63.12 (s, 6 F, *para*-CF₃), −59.73 (s, 12 F, *ortho*-CF₃) ppm. ¹H NMR: δ = 2.22 [s, 6 H, NC₅H₄(CH₃)], 6.76 [d, *J* = 6.5 Hz, 4 H, NC₅H₄(CH₃)], 7.82 [s, 4 H, C₆H₂(CF₃)₃], 7.92 [d, *J* = 6.5 Hz, 4 H, NC₅H₄(CH₃)] ppm. C₃₀H₁₈F₁₈N₂Pd (854.86): calcd. C 42.15, H 2.12, N 3.28; found C 42.27, H 2.38, N 3.50.

***trans*-[Pd(Fmes)₂(PMe₃)₂] (**1d**):** In a Young-valve-fitted Schlenk flask, PMe₃ (200 μ L of 1 M in THF, 0.2 mmol) was added to a solution of **1a** (0.080 g, 0.1 mmol) in toluene (10 mL) and heated to 110 °C for 7 h. Work up as for **1c** then yielded 0.028 g (34%) of material. Recrystallization from dichloromethane/hexane gave colourless crystals. IR: $\tilde{\nu}$ = 688 s cm^{−1}. ¹⁹F NMR: δ = −63.13 (s, 6 F, *para*-CF₃), −59.51 (t, *J* = 5.5 Hz, 12 F, *ortho*-CF₃) ppm. ³¹P{¹H} NMR: δ = −20.12 (sept, *J* = 5.5 Hz) ppm. ¹H NMR: δ = 0.83 [A₉XX'A₉' syst., *J* = 7 Hz, 18 H, P(CH₃)₃], 7.89 [s, 4 H, C₆H₂(CF₃)₃] ppm. C₂₄H₂₂F₁₈P₂Pd (820.76): calcd. C 35.12, H 2.7, found C 34.86, H 2.59.

***trans*-[Pd(Fmes)₂(*t*BuNC)₂] (**1e**):** *t*BuNC (225 μ L, 0.165 g, 2 mmol) was added to a solution of **1a** (0.080 g, 0.1 mmol) in toluene (10 mL) and boiled under reflux for 5 h. Work up as for **1c** subsequently yielded 0.070 g (83%) of material. Recrystallization from dichloromethane/hexane gave colourless crystals. IR: $\tilde{\nu}$ = 686 s cm^{−1}. ¹⁹F NMR: δ = −63.00 (s, 6 F, *para*-CF₃), −61.74 (s, 12 F, *ortho*-CF₃) ppm. ¹H NMR: δ = 1.16 (s, 18 H, CNC₄H₉), 7.92 [s, 4 H, C₆H₂(CF₃)₃] ppm. C₂₈H₂₂F₁₈N₂Pd (834.87): calcd. C 40.28, H 2.66, N 3.36; found C 40.27, H 2.61, N 3.21.

***trans*-[Pd(Fmes)₂(*p*Tol-NC)₂] (**1f**):** *p*Tol-NC (0.100 g, 0.85 mmol) was added to a solution of **1a** (0.160 g, 0.2 mmol) in toluene (15 mL) and boiled under reflux for 8 h. Subsequent work up as for **1c** yielded 0.045 g (28%) of material. Recrystallization from di-

chloromethane/ethanol gave colourless crystals. IR: $\tilde{\nu}$ = 2197 s (v CN), 688 s cm^{-1} . ^{19}F NMR: δ = -63.07 (s, 6 F, *para*-CF₃), -61.64 (s, 12 F, *ortho*-CF₃) ppm. ^1H NMR: δ = 2.31 (s, 18 H, CNC₄H₉), 7.01 (part B of AB system, J = 8.4 Hz, 4 H), 7.10 (part A, J = 8.4 Hz, 4 H), 7.96 [s, 4 H, C₆H₂(CF₃)₃] ppm. C₃₄H₁₈F₁₈N₂Pd (902.91): calcd. C 45.23, H 2.01, N 3.10; found C 44.93, H 2.18, N 3.21.

trans-[Pd(Fmes)₂(NCMe)(SMe₂)] (2a): **1a** (0.080 g, 0.1 mmol) was dissolved in acetonitrile (15 mL) and boiled under reflux for 7 h. Work up as for **1c** yielded then afforded 0.042 g (54%) of material. Recrystallization from dichloromethane/hexane gave pale yellow crystals. IR: $\tilde{\nu}$ = 686 m cm^{-1} . ^{19}F NMR: δ = -63.08 (s, 6 F, *para*-CF₃), -60.51 (s, 12 F, *ortho*-CF₃) ppm. ^1H NMR: δ = 1.61 [s, 6 H, S(CH₃)₂], 1.99 (s, 3 H, NCCH₃), 7.90 [s, 4 H, C₆H₂(CF₃)₃] ppm. C₂₂H₁₃F₁₈NPdS (771.79): calcd. C 34.24, H 1.70, N 1.81; found C 34.17, H 1.85, N 1.85.

trans-[Pd(Fmes)₂(NCMe)(tht)] (2b): **1b** (0.127 g, 0.15 mmol) was dissolved in acetonitrile (15 mL) and boiled under reflux for 24 h. Subsequent work up as for **1c** yielded 0.042 g (35%) and recrystallization from dichloromethane/hexane gave yellow crystals. IR: $\tilde{\nu}$ = 688 m cm^{-1} . ^{19}F NMR: δ = -63.06 (s, 6 F, *para*-CF₃), -60.21 (s, 12 F, *ortho*-CF₃) ppm. ^1H NMR: δ = 1.70 (m, 4 H, H ^{β} , SC₄H₈), 1.99 (s, 3 H, NCCH₃), 2.21 (m, 4 H, H ^{α} , SC₄H₈), 7.89 [s, 4 H, C₆H₂(CF₃)₃] ppm. C₂₄H₁₆F₁₈NPdS (798.83): calcd. C 36.13, H 1.90, N 1.76; found C 36.07, H 1.94, N 2.10.

NnBu₄[trans-Pd(Fmes)₂I(SMe₂)] (3a): NnBu₄I (0.037 g, 0.1 mmol) was added to a solution of **1a** (0.080 g, 0.1 mmol) in toluene (10 mL) and boiled under reflux for 2 h. Work up as for **1c** yielded 0.047 g (43%), and subsequent recrystallization from dichloromethane/hexane gave orange crystals. IR: $\tilde{\nu}$ = 687 s, 666 w cm^{-1} . ^{19}F NMR: δ = -62.74 (s, 6 F, *para*-CF₃), -58.33 (s, 12 F, *ortho*-CF₃) ppm. ^1H NMR: δ = 0.93 [m, 12 H, Nn(C₄H₉)₄], 1.31 [m, 8 H, Nn(C₄H₉)₄], 1.51 [m, 8 H, Nn(C₄H₉)₄], 1.64 [s, 6 H, S(CH₃)₂], 3.03 [m, 8 H, Nn(C₄H₉)₄], 7.77 [s, 4 H, C₆H₂(CF₃)₃] ppm. C₃₆H₄₆F₁₈INPdS (1100.110): calcd. C 39.31, H 4.21, N 1.27; found C 39.52, H 4.18, N 1.52.

NnBu₄[trans-Pd(Fmes)₂I(tht)] (3b): NnBu₄I (0.037 g, 0.1 mmol) was added to a solution of **1b** (0.084 g, 0.1 mmol) in toluene (10 mL) and boiled under reflux for 6 h. Work up as for **1c** then yielded 0.036 g (32%), and subsequent recrystallization from dichloromethane/hexane gave orange crystals. IR: $\tilde{\nu}$ = 687 s, 663 w. ^{19}F NMR: δ = -62.73 (s, 6 F, *para*-CF₃), -58.01 (s, 12 F, *ortho*-CF₃) ppm. ^1H NMR: δ = 0.92 [m, 12 H, Nn(C₄H₉)₄], 1.28 [m, 8 H, Nn(C₄H₉)₄], 1.48 [m, 8 H, Nn(C₄H₉)₄], 1.70 [m, 4 H, Nn(C₄H₉)₄], 2.28 [m, 4 H, SCH₂], 3.03 [m, 8 H, Nn(C₄H₉)₄], 7.76 [s, 4 H, C₆H₂(CF₃)₃] ppm. C₃₈H₄₈F₁₈INPdS (1126.15): calcd. C 40.53, H 4.30, N 1.24; found C 40.38, H 4.11, N 1.27.

[Pd(Fmes)₂(Me₂bipy)] (4a): Me₂bipy (0.022 g, 0.12 mmol) was added to a solution of **1a** (0.080 g, 0.1 mmol) in toluene (10 mL) and boiled under reflux for 7 h. Work up as for **1c** then yielded 0.067 g (79%) of material. Recrystallization from acetone/hexane then afforded yellow crystals. IR: $\tilde{\nu}$ = 692 s, 685 s cm^{-1} . ^{19}F NMR: δ = -63.10 (s, 6 F, *para*-CF₃), -57.73 (s, 12 F, *ortho*-CF₃) ppm. ^1H NMR: δ = 2.51 [s, 6 H, {NC₅H₃(CH₃)₂}], 7.11 [d, J = 5.4 Hz, 2 H, {NC₅H₃(CH₃)₂}], 7.44 [d, J = 5.4 Hz, 2 H, {NC₅H₃(CH₃)₂}], 7.77 [s, 4 H, C₆H₂(CF₃)₃], 7.88 [s, 2 H, H³, {NC₅H₃(CH₃)₂}] ppm. C₃₀H₁₆F₁₈N₂Pd (852.85): calcd. C 42.25, H 1.89, N 3.28; found C 41.56, H 2.16, N 3.20.

[Pd(Fmes)₂(biquinoly)] (4b): 2,2'-Biquinoline (0.026 g, 0.1 mmol) was added to a solution of **1a** (0.080 g, 0.1 mmol) in toluene

(10 mL) and boiled under reflux for 15 h; work up as for **1c** then yielded 0.053 g (57%). Subsequent recrystallization from toluene/hexane then gave yellow crystals. IR: $\tilde{\nu}$ = 686 m, 669 m cm^{-1} . ^{19}F NMR: δ = -63.23 (s, 6 F, *para*-CF₃), -57.99 (br., 12 F, *ortho*-CF₃) ppm. ^1H NMR: δ = 7.29 [t, J = 7 Hz, 2 H, (NC₉H₆)₂], 7.53 [t, J = 7 Hz, 2 H, (NC₉H₆)₂], 7.66 [s, 4 H, C₆H₂(CF₃)₃], 7.82 [d, J = 8.5 Hz, 2 H, (NC₉H₆)₂], 7.87 [d, J = 8.5 Hz, 2 H, (NC₉H₆)₂], 8.30 [d, J = 8.5 Hz, 2 H, (NC₉H₆)₂], 8.58 [d, J = 8.5 Hz, 2 H, (NC₉H₆)₂] ppm. ^{19}F NMR (CD₂Cl₂, 183 K): δ = -62.43 (s, 6 F, *para*-CF₃), -59.10 (br., 6 F, *ortho*-CF₃), -55.89 (br., 6 F, *ortho*-CF₃) ppm. ^1H NMR (CD₂Cl₂, 183 K): δ = 7.31 [t, J = 7 Hz, 2 H, (NC₉H₆)₂], 7.49 [t, 2 H, J = 7 Hz, (NC₉H₆)₂], 7.66 [m, 8 H, C₆H₂(CF₃)₃ and N₂C₁₈H₁₂], 8.24 [d, 2 H, J = 7 Hz, (NC₉H₆)₂], 8.44 [d, J = 8 Hz, 2 H, (NC₉H₆)₂] ppm. C₃₆H₁₆F₁₈N₂Pd (924.91): calcd. C 46.75, H 1.74, N 3.03; found C 46.45, H 1.87, N 2.96.

[Pd(Fmes)₂(κ²N,N'-OCPy₂)] (4c): OCPy₂ (0.018 g, 1 mmol) was added to a solution of **1a** (0.080 g, 0.1 mmol) in toluene (10 mL) and boiled under reflux for 3 h. Subsequent work up as for **1c** yielded 0.020 g (47%), and recrystallization from toluene/hexane then gave yellow crystals. IR: $\tilde{\nu}$ = 693 m, 686 s cm^{-1} . ^{19}F NMR: δ = -63.28 (s, 6 F, *para*-CF₃), -57.70 (s, 12 F, *ortho*-CF₃) ppm. ^1H NMR: δ = 7.41 [m, 2 H, OC(NC₅H₄)₂], 7.69 [s, 4 H, C₆H₂(CF₃)₃], 8.04 [m, 2 H, OC(NC₅H₄)₂], 8.22 [m, 4 H, OC(NC₅H₄)₂] ppm. C₂₉H₁₂F₁₈N₂OPd (852.80): calcd. C 40.84, H 1.42, N 3.28; found C 40.95, H 1.60, N 3.48.

[Pd(Fmes)₂(dppm)] (4d): The ligand dppm (0.046 g, 0.12 mmol) was added to a solution of **1a** (0.080 g, 0.1 mmol) in toluene (10 mL) and boiled under reflux for 7 h. Work up as for **1c** then yielded 0.063 g (60%), and subsequent recrystallization from toluene/hexane gave yellow crystals. IR: $\tilde{\nu}$ = 693 s, 664 w cm^{-1} . ^{19}F NMR: δ = -63.19 (s, 6 F, *para*-CF₃), -57.25 (X₆AA'X₆' syst., N = J_{AX} + J_{AX'} = 11.9 Hz, 12 F, *ortho*-CF₃) ppm. $^{31}\text{P}\{^1\text{H}\}$ NMR: δ = -36.85 (m) ppm. ^1H NMR: δ = 4.18 [t, J = 9.5 Hz, 2 H, {(C₆H₅)₂P}CH₂], 7.20 [m, 15 H, {(C₆H₅)₂P}CH₂], 7.38 [m, 5 H, {(C₆H₅)₂P}CH₂], 7.64 [s, 4 H, C₆H₂(CF₃)₃] ppm. C₄₃H₂₆F₁₈P₂Pd (1053.01): calcd. C 49.05, H 2.49; found C 49.59, H 2.69.

[Pd(Fmes)₂(dppe)] (4e): The ligand dppe (0.044 g, 0.11 mmol) was added to a solution of **1a** (0.080 g, 0.1 mmol) in toluene (10 mL) and boiled under reflux for 3 h. Subsequent work up as for **1c** afforded 0.080 g (75%), and recrystallization from toluene/hexane then gave colourless crystals. IR: $\tilde{\nu}$ = 689 s, 665 m cm^{-1} . ^{19}F NMR: δ = -63.26 (s, 6 F, *para*-CF₃), -56.90 (X₆AA'X₆' syst., N = J_{AX} + J_{AX'} = 11.2 Hz, 12 F, *ortho*-CF₃) ppm. $^{31}\text{P}\{^1\text{H}\}$ NMR: δ = 35.62 (m) ppm. ^1H NMR: δ = 2.54 (X₂AA'X₂' syst., N = J_{AX} + J_{AX'} = 18.4 Hz, CH₂, 4 H), 7.35 (m, C₆H₅, 5 H), 7.24 (m, C₆H₅, 15 H), 7.52 [s, C₆H₂(CF₃)₃, 4 H], 7.35 (m, C₆H₅, 5 H) ppm. C₄₄H₂₈F₁₈P₂Pd (1067.03): calcd. C 49.53, H 2.64; found C 49.90, H 2.85.

[Pd(Fmes)₂(pte)] (4f): The ligand pte (0.016 g, 0.065 mmol) was added to a solution of **1a** (0.040 g, 0.05 mmol) in toluene (10 mL) and boiled under reflux for 5 h. The usual work up, as for **1c**, then yielded 0.015 g (33%), and subsequent recrystallization from toluene/hexane gave yellow crystals. IR: $\tilde{\nu}$ = 685 s, 664 m cm^{-1} . ^{19}F NMR: δ = -63.38 (s, 6 F, *para*-CF₃), -56.23 (br., 12 F, *ortho*-CF₃) ppm. ^1H NMR: δ = 3.42 (s, 4 H, CH₂), 7.35 (m, 10 H, C₆H₅), 7.65 (br., 4 H, C₆H₅) ppm. ^{19}F NMR (213 K): δ = -62.86 (s, 6 F, *para*-CF₃), -59.50 (br., 6 F, *ortho*-CF₃), -52.50 (br., 6 F, *ortho*-CF₃) ppm. ^1H NMR (213 K): δ = 3.38 (s, 4 H, CH₂), 7.37 (m, 10 H, C₆H₅), 7.56 [br., 2 H, C₆H₂(CF₃)₃], 7.78 [br., 2 H, C₆H₂(CF₃)₃] ppm. C₃₂H₁₈F₁₈PdS₂ (914.99): calcd. C 42.01, H 1.98; found C 41.81, H 2.16.

[Pd(Fmes)₂(κ²S,N-SPPPh₂Py)] (5a): SPPPh₂Py (0.033 g, 0.11 mmol) was added to a solution of **1a** (0.080 g, 0.1 mmol) in toluene (10 mL) and boiled under reflux for 4 h. The usual work up, as for **1c**, then yielded 0.069 g (72%), and recrystallization from toluene/hexane then gave yellow crystals. IR: $\tilde{\nu}$ = 688 s, 664 vw cm⁻¹. ¹⁹F NMR: δ = -63.18 (s, 3 F, *para*-CF₃), -63.12 (s, 3 F, *para*-CF₃), -58.11 (q, *J*_{F,F} = 9.3 Hz, 6 F, *ortho*-CF₃), -56.34 (q, *J*_{F,F} = 9.3 Hz, 6 F, *ortho*-CF₃) ppm. ³¹P{¹H} NMR: δ = 57.05 (s) ppm. ¹H NMR: δ = 7.35 [m, 2 H, SP(C₆H₅)₂(NC₅H₄)], 7.67 [s, 2 H, C₆H₂(CF₃)₃], 7.68 [s, 2 H, C₆H₂(CF₃)₃], 7.70 [m, 10 H, SP(C₆H₅)₂(NC₅H₄)], 7.87 [m, 1 H, SP(C₆H₅)₂(NC₅H₄)], 7.99 [m, 1 H, SP(C₆H₅)₂(NC₅H₄)] ppm. C₃₅H₁₈F₁₈NPPdS (963.95): calcd. C 43.61, H 1.88, N 1.45; found C 43.53, H 1.94, N 1.40.

[Pd(Fmes)₂(κ²O,N-OPPhPy₂)] (5b): OPPhPy₂ (0.031 g, 0.11 mmol) was added to a solution of **1a** (0.080 g, 0.1 mmol) in toluene (10 mL) and boiled under reflux for 2 h. The usual work up, as for **1c**, yielded 0.056 g (59%) of material. Subsequent recrystallization from toluene/hexane then gave yellow crystals. IR: $\tilde{\nu}$ = 685 s, 665 w cm⁻¹. ¹⁹F NMR: δ = -63.17 (s, 3 F, *para*-CF₃), -63.16 (s, 3 F, *para*-CF₃), -58.23 (q, *J*_{F,F} = 7.5 Hz, 3 F, *ortho*-CF₃), -57.55 (q, *J*_{F,F} = 6 Hz, 3 F, *ortho*-CF₃), -57.28 (q, *J*_{F,F} = 6 Hz, 3 F, *ortho*-CF₃), -56.28 (q, *J*_{F,F} = 7.5 Hz, 3 F, *ortho*-CF₃) ppm. ³¹P{¹H} NMR: δ = 39.02 (s) ppm. ¹H NMR: δ = 7.34 [m, 1 H, OP(C₆H₅)(NC₅H₄)₂], 7.58 [m, 4 H, OP(C₆H₅)(NC₅H₄)₂], 7.68 [m, 1 H, OP(C₆H₅)(NC₅H₄)₂], 7.70 [s, 1 H, C₆H₂(CF₃)₃], 7.72 [s, 1 H, C₆H₂(CF₃)₃], 7.76 [s, 1 H, C₆H₂(CF₃)₃], 7.79 [s, 1 H, C₆H₂(CF₃)₃], 7.91 [m, 1 H, OP(C₆H₅)(NC₅H₄)₂], 8.00 [m, 1 H, OP(C₆H₅)(NC₅H₄)₂], 8.11 [m, 3 H, OP(C₆H₅)(NC₅H₄)₂], 8.37 [t, *J* = 7 Hz, 1 H, OP(C₆H₅)(NC₅H₄)₂], 8.88 [d, *J* = 4.7 Hz, 1 H, OP(C₆H₅)(NC₅H₄)₂] ppm. C₃₄H₁₇F₁₈N₂OPPd (948.87): calcd. C 43.03, H 1.81, N 2.95; found C 43.42, H 1.98, N 2.96.

[Pd(Fmes)₂(μ-1κN:1,2κO:2κN-Py₂MeCO)Pd(Fmes)(SMe₂)] (6): (OH)(CH₃)Cpy₂ (225 μL, 0.010 g, 0.05 mmol) was added to a solution of **1a** (0.080 g, 0.1 mmol) in toluene (10 mL) and boiled under reflux for 11 h. The usual work up, as for **1c**, then yielded 0.022 g (33%), and subsequent recrystallization from toluene gave yellow crystals. IR: $\tilde{\nu}$ = 694 s, 685 s cm⁻¹. ¹⁹F NMR: δ = -63.21 (s, 3 F, *para*-CF₃), -63.11 (s, 3 F, *para*-CF₃), -63.07 (s, 3 F, *para*-CF₃), -61.70 (q, *J* = 8.8 Hz, 3 F, *ortho*-CF₃), -60.75 (s, 3 F, *ortho*-CF₃), -59.52 (q, *J* = 8.0 Hz, 3 F, *ortho*-CF₃), -59.12 (qq, *J* = 8.5, 10.0 Hz, 3 F, *ortho*-CF₃), -57.88 (q, *J* = 10.0 Hz, 3 F, *ortho*-CF₃), -53.53 (q, *J* = 8.0 Hz, 3 F, *ortho*-CF₃) ppm. ¹H NMR: δ = 1.09 [br., 3 H, S(CH₃)₂], 2.36 [br., 3 H, S(CH₃)₂], 2.53 (s, 3 H, CH₃), 6.62 (d, *J* = 8.0 Hz, 1 H, C₅H₄N), 7.09 (t, *J* = 6.0 Hz, 1 H, C₅H₄N), 7.17 (t, *J* = 6.0 Hz, 1 H, C₅H₄N), 7.29 (d, *J* = 5.2 Hz, 1 H, C₅H₄N), 7.61 [s, 1 H, C₆H₂(CF₃)₃], 7.63 [s, 1 H, C₆H₂(CF₃)₃], 7.67 [m, 2 H, C₆H₂(CF₃)₃, C₅H₄N], 7.71 [s, 1 H, C₆H₂(CF₃)₃], 7.85 [s, 1 H, C₆H₂(CF₃)₃], 7.94 [m, 2 H, C₆H₂(CF₃)₃ and C₅H₄N] ppm. C₄₁H₂₃F₂₇N₂Pd₂OS (1317.47): calcd. C 37.38, H 1.76, N 2.17; found C 37.67, H 1.89, N 2.17.

X-ray Crystallographic Study: Suitable crystals of **1f** and **4b** were grown by slow diffusion of a concentrated dichloromethane solution of the complex into diethyl ether (**1f**) or n-hexane (**4b**) at -20 °C. For **6**·0.5 toluene, crystals were grown by slow evaporation of a concentrated toluene solution of the complex at 8 °C. X-ray measurements were made using a Bruker SMART CCD area-detector diffractometer with Mo-K_α radiation (λ = 0.71073 Å).^[35] Intensities were integrated from several series of exposures,^[36] each exposure covering 0.3° in ω , the total data set being a hemisphere. Absorption corrections were applied, based on multiple and symmetry-equivalent measurements.^[37] The structure was solved by direct methods and refined by least-squares on weighted *F*² values for

Table 5. Crystal data and structure refinement for *trans*-[Pd(Fmes)₂(*p*Tol-NC)₂] (**1f**), [Pd(Fmes)₂(biquinolyl)] (**4b**), and [Pd(Fmes)₂(μ-1κN:1,2κO:2κN-Py₂MeCO)Pd(Fmes)(SMe₂)](C₆H₅CH₃)_{0.5} (**6**·0.5 toluene)

	1f	4b	6 ·0.5 toluene
Empirical formula	C ₃₄ H ₁₈ F ₁₈ N ₂ Pd	C ₃₆ H ₁₆ F ₁₈ N ₂ Pd	C _{44.5} H ₂₇ F ₂₇ N ₂ OPd ₂ S
Molecular mass	902.90	924.91	1363.54
Temperature	298(2) K	293(2) K	293(2)
Wavelength (Å)	0.71073	0.71073	0.71073
Crystal system	triclinic	triclinic	triclinic
Space group	<i>P</i> $\bar{1}$	<i>P</i> $\bar{1}$	<i>P</i> $\bar{1}$
<i>a</i> (Å)	9.262(5)	11.5004(13)	15.400(4)
<i>b</i> (Å)	12.424(6)	11.9885(14)	18.748(5)
<i>c</i> (Å)	16.720(8)	13.7943(15)	20.396(5)
α (deg)	95.169(10)	77.804(3)	62.940(5)
β (deg)	102.807(10)	67.306(2)	79.447(6)
γ (deg)	105.098(9)	75.890(2)	81.438(7)
<i>V</i> (Å ³)	1788.9(15)	1687.0(3)	5141(2)
<i>Z</i>	2	2	4
<i>D</i> _{calcd.} (g cm ⁻³)	1.676	1.821	1.762
Absorption coefficient (mm ⁻¹)	0.640	0.682	0.875
<i>F</i> (000)	888	908	2668
Crystal size (mm)	0.29 × 0.16 × 0.15	0.12 × 0.12 × 0.06	0.39 × 0.12 × 0.05
Theta range for data collection	1.26 to 23.28°	1.61 to 23.29°	1.13 to 23.32°
Reflections collected	8283	7906	24237
Independent reflections	5091 (<i>R</i> _{int} = 0.0180)	4838 (<i>R</i> _{int} = 0.0400)	14733 (<i>R</i> _{int} = 0.0531)
Absorption correction	SADABS	SADABS	SADABS
Maximum and minimum transmission factor	1.000000, 0.876647	1.000000, 0.652705	1.000000, 0.631134
Data/restraints/parameters	5091/0/501	4838/0/514	14733/0/1353
Goodness-of-fit on <i>F</i> ²	1.050	1.006	1.015
<i>R</i> _I [<i>I</i> > 2σ(<i>I</i>)]	0.0363	0.0474	0.0611
<i>wR</i> ₂ (all data)	0.1074	0.1040	0.1926

all reflections (Table 5).^[38] All non-hydrogen atoms were assigned anisotropic displacement parameters and refined without positional constraints, except that the carbon atoms of the toluene molecule in **6**·0.5 toluene were refined isotropically. Hydrogen atoms were constrained to ideal geometries and refined with fixed isotropic displacement parameters. Refinement proceeded smoothly to give the residuals shown in Table 5. Complex neutral-atom scattering factors were used.^[39] CCDC-221232 (for **1f**), -221233 (for **4b**) and -221234 (for **6**·0.5 toluene) contain the supplementary crystallographic data for this paper. These data can be obtained free of charge at www.ccdc.cam.ac.uk/conts/retrieving.html [or from the Cambridge Crystallographic Data Centre, 12 Union Road, Cambridge CB2 1EZ, UK; Fax: (internat.) +44-1223-336-033; E-mail: deposit@ccdc.cam.ac.uk].

Acknowledgments

The authors thank the DGI (BQU2001–2015) and the JCyL (VA058/03) for financial support.

- [1] See, for example: [1a] F. T. Edelmann, *Comments, Inorg. Chem.* **1992**, *12*, 259–284, and references cited therein. [1b] A. S. Batsanov, K. B. Dillon, V. C. Gibson, J. A. K. Howard, L. J. Sequeira, J. W. Yao, *J. Organomet. Chem.* **2001**, *631*, 181–187. [1c] K. B. Dillon, V. C. Gibson, J. A. K. Howard, L. J. Sequeira, J. W. Yao, *J. Organomet. Chem.* **1997**, *528*, 179–183. [1d] V. C. Gibson, C. Redshaw, L. J. Sequeira, K. B. Dillon, W. Clegg, J. M. R. Elsegood, *Chem. Commun.* **1996**, 2151–2152. [1e] R. D. Schluter, A. H. Cowley, D. A. Atwood, R. A. Jones, M. R. Bond, C. J. Carrano, *J. Am. Chem. Soc.* **1993**, *115*, 2070–2071. [1f] P. Espinet, S. Martín-Barrios, F. Villafañe, P. G. Jones, A. K. Fischer, *Organometallics* **2000**, *19*, 290–295.
- [2] [2a] C. Bartolomé, P. Espinet, F. Villafañe, S. Giesa, A. Martín, A. G. Orpen, *Organometallics* **1996**, *15*, 2019–2028. [2b] C. Bartolomé, R. de Blas, P. Espinet, J. M. Martín-Álvarez, F. Villafañe, *Angew. Chem. Int. Ed.* **2001**, *40*, 2521–2524. [2c] C. Bartolomé, P. Espinet, J. M. Martín-Álvarez, F. Villafañe, *Eur. J. Inorg. Chem.* **2003**, 3127–3138. [2d] C. Bartolomé, P. Espinet, J. M. Martín-Álvarez, F. Villafañe, *Inorg. Chim. Acta* **2003**, *347*, 49–52. [2e] C. Bartolomé, P. Espinet, L. Vicente, F. Villafañe, J. P. H. Charmant, A. G. Orpen, *Organometallics* **2002**, *21*, 3536–3543.
- [3] [3a] A. C. Albéniz, A. L. Casado, P. Espinet, *Organometallics* **1997**, *16*, 5416–5423. [3b] A. C. Albéniz, A. L. Casado, P. Espinet, *Inorganic Chemistry* **1999**, *38*, 2510–2515. [3c] M. A. Alonso, J. A. Casares, P. Espinet, J. M. Martínez-Ilarduya, C. Pérez-Briso, *Eur. J. Inorg. Chem.* **1998**, 1745–1753.
- [4] [4a] R. Usón, J. Fornies, *Adv. Organomet. Chem.* **1988**, *28*, 219–297. [4b] M. P. García, M. V. Jiménez, F. S. Lahoz, L. A. Oro, *Inorg. Chem.* **1995**, *34*, 2153–2159. [4c] J. M. Casas, F. A. Cotton, L. R. Falvello, J. Fornies, A. Martín, M. Tomás, R. Usón, *J. Am. Chem. Soc.* **1994**, *116*, 7160–7165. [4d] L. R. Falvello, J. Fornies, C. Fortuño, F. Martínez, *Inorg. Chem.* **1994**, *33*, 6242–6246. [4e] J. Casabó, G. García, G. López, C. Miravittles, E. Molins, J. Ruiz, C. Vicente, *Inorg. Chem.* **1991**, *30*, 2605–2610. [4f] G. B. Deacon, K. T. Nelson-Reed, *J. Organomet. Chem.* **1987**, *322*, 257–268. [4g] R. Usón, A. Laguna, *Coord. Chem. Rev.* **1986**, *70*, 1–50.
- [5] J. A. Casares, P. Espinet, J. M. Martínez-Ilarduya, Y. S. Lin, *Organometallics* **1997**, *16*, 770–779.
- [6] F. T. Edelmann, M. Belay, *J. Fluorine Chem.* **1997**, *84*, 29–33.
- [7] [7a] P. Espinet, J. M. Martínez-Ilarduya, C. Pérez-Briso, A. L. Casado, M. A. Alonso, *J. Organomet. Chem.* **1998**, *551*, 9–20. [7b] G. López, G. García, M. D. Santana, G. Sánchez, J. Ruiz, J. A. Hermoso, A. Vegas, M. Martínez-Ripoll, *J. Chem. Soc., Dalton Trans.* **1990**, 1621–1626.
- [8] [8a] P. G. Jones, *J. Organomet. Chem.* **1988**, *345*, 405–411. [8b] A. Domenicano, A. Vaciago, C. A. Coulson, *Acta Crystallogr., Sect. B* **1975**, *31*, 221–234. [8c] A. Domenicano, P. Murray-Rust, A. Vaciago, *Acta Crystallogr., Sect. B* **1983**, *39*, 457–468 and references cited therein. [8d] R. Norrestam, L. Schepper, *Acta Chem. Scand., Ser. A* **1981**, *35*, 91–103. [8e] A. Domenicano, P. Mazzeo, A. Vaciago, *Tetrahedron Lett.* **1976**, 1029–1032.
- [9] [9a] S. Coco, P. Espinet, F. Mayor, X. Solans, *J. Chem. Soc., Dalton Trans.* **1991**, 2503–2509. [9b] P. Leoni, E. Vichi, S. Lenconi, M. Pasquali, E. Chiarentin, A. Albinati, *Organometallics* **2000**, *19*, 3062–3068. [9c] S. Cristofani, P. Leoni, M. Pasquali, F. Eisentraeger, A. Albinati, *Organometallics* **2000**, *19*, 4589–4595.
- [10] [10a] A. J. Deeming, I. P. Rothwell, *J. Chem. Soc., Chem. Commun.* **1979**, 670–672. [10b] A. Albinati, C. Ammann, P. S. Pregosin, H. Rüegger, *Organometallics* **1990**, *9*, 1826–1833.
- [11] C. Bartolomé, R. de Blas, P. Espinet, F. Villafañe, manuscript in preparation.
- [12] [12a] K. Nakamoto, *Infrared and Raman Spectra of Inorganic and Coordination Compounds*, 3rd ed. John Wiley & Sons, New York, **1978**. [12b] T. S. Lobana, *Prog. Inorg. Chem.* **1989**, *37*, 495.
- [13] A. J. Canty, L. A. Titcombe, B. W. Skelton, A. H. White, *J. Chem. Soc., Dalton Trans.* **1988**, 35–45.
- [14] A. Basu, S. Bhaduri, N. Y. Sapre, P. G. Jones, *J. Chem. Soc., Chem. Commun.* **1987**, 1724–1725.
- [15] See, for example: M. A. Bennett, G. B. Robertson, A. Rokicki, W. A. Wickramasinghe, *J. Am. Chem. Soc.* **1988**, *110*, 7098–7105, and references cited therein.
- [16] R. J. Cross, *Adv. Inorg. Chem.* **1989**, *34*, 219–291.
- [17] [17a] U. Frey, L. Helm, A. E. Merbach, R. Romeo, *J. Am. Chem. Soc.* **1989**, *111*, 8161–8165, and references cited therein. [17b] S. Lanza, D. Minniti, P. Moore, J. Sachindis, R. Romeo, M. Tobe, *Inorg. Chem.* **1984**, *23*, 4428–4433. [17c] R. Romeo, A. Grassi, L. M. Scolaro, *Inorg. Chem.* **1992**, *31*, 4383–4390. [17d] G. Alibrandi, L. M. Scolaro, R. Romeo, *Inorg. Chem.* **1991**, *30*, 4007–4013, and references cited therein. [17e] R. Romeo, *Comments, Inorg. Chem.* **1990**, *11*, 21–57 and references cited therein.
- [18] [18a] R. Usón, A. Laguna, J. Vicente, J. García, P. G. Jones, G. M. Sheldrick, *J. Chem. Soc., Dalton Trans.* **1981**, 655–657. [18b] P. G. Jones, *Naturforsch., B* **1982**, *37*, 937–940.
- [19] G. M. Benedikt, B. L. Goodall, S. Iyer, L. H. McIntosh III, R. Mimna, L. F. Rhodes, C. S. Day, V. W. Day, *Organometallics* **2001**, *20*, 2565–2569.
- [20] J. A. Casares, S. Coco, P. Espinet, Y. S. Lin, *Organometallics* **1995**, *14*, 3058–3067.
- [21] L. Ernst, K. Ibrom, *Angew. Chem. Int. Ed. Engl.* **1995**, *34*, 1881–1882.
- [22] [22a] D. Minniti, *Inorg. Chem.* **1994**, *33*, 2631–2634. [22b] A. L. Casado, J. A. Casares, P. Espinet, *Inorg. Chem.* **1998**, *37*, 4154–4156.
- [23] [23a] R. H. Crabtree, *The Organometallic Chemistry of the Transition Elements*, 2nd ed., John Wiley & Sons, New York, **1994**. [23b] A. Yamamoto, *Organotransition Metal Chemistry. Fundamental Concepts and Applications*, John Wiley & Sons, New York, **1986**.
- [24] [24a] J. Vicente, A. Arcas, D. Bautista, *Organometallics* **1997**, *16*, 2127–2138. [24b] J. Vicente, J. A. Abad, A. D. Frankland, M. C. Ramírez de Arellano, *Chem. Eur. J.* **1999**, *5*, 3066–3075. [24c] J. Vicente, J. A. Abad, E. Martínez-Viviente, P. G. Jones, *Organometallics* **2002**, *21*, 4454–4467. [24d] J. Vicente, A. Arcas, D. Bautista, M. C. Ramírez de Arellano, *J. Organomet. Chem.* **2002**, *663*, 164–172.
- [25] R. Usón, J. Fornies, F. Martínez, M. Tomás, I. Reoyo, *Organometallics* **1983**, *2*, 1386–1390.
- [26] P. Espinet, R. Hernando, G. Iturbe, A. G. Orpen, I. Pascual, F. Villafañe, *Eur. J. Inorg. Chem.* **2000**, 1031–1038.
- [27] D. D. Perrin, W. L. F. Armarego, *Purification of Laboratory Chemicals*, 3rd ed.; Pergamon Press: Oxford, U. K., **1988**.

- [28] R. Usón, J. Forniés, F. Martínez, M. Tomás, *J. Chem. Soc., Dalton Trans.* **1980**, 888–894.
- [29] G. R. Newkome, D. C. Hager, *J. Org. Chem.* **1978**, *43*, 947–949.
- [30] F. G. Mann, J. Watson, *J. Org. Chem.* **1948**, *13*, 502–531.
- [31] Treatment of OCPy₂ with LiMe and further hydrolysis affords (OH)(CH₃)CPy₂, which can be recrystallized from dichloromethane/hexane. Spectroscopic data agree with those previously reported: S. Bhaduri, N. Y. Sapre, P. G. Jones, *J. Chem. Soc., Dalton Trans.* **1991**, 2539–2543.
- [32] I. Ugi, R. Meyr, *Chem. Ber.* **1960**, *93*, 239–248.
- [33] H. Eckert, B. Forster, *Angew. Chem. Int. Ed. Engl.* **1987**, *26*, 894–895.
- [34] [34a] G. E. Carr, R. D. Chambers, T. F. Holmes, D. G. Parker, *J. Organomet. Chem.* **1987**, *325*, 13–23. [34b] M. Scholz, H. W. Roesky, D. Stalke, K. Keller, F. T. Edelmann, *J. Organomet. Chem.* **1989**, *366*, 73–85.
- [35] SMART V5.051 diffractometer control software, Bruker Analytical X-ray Instruments Inc., Madison, WI, **1998**.
- [36] SAINT V6.02 integration software, Siemens Analytical X-ray Instruments Inc., Madison, WI, **1999**.
- [37] G. M. Sheldrick. *SADABS: A program for absorption correction with the Siemens SMART system*; University of Göttingen: Germany, **1996**.
- [38] *SHELXTL program system version 5.1*; Bruker Analytical X-ray Instruments Inc., Madison, WI **1998**.
- [39] *International Tables for Crystallography*, Kluwer, Dordrecht, **1992**, vol. C.

Received October 20, 2003

Early View Article

Published Online April 7, 2004